Am J Physiol Regul Integr Comp Physiol 302: R1313–R1326, 2012.
First published April 4, 2012; doi:10.1152/ajpregu.00086.2012.

Leptin-sensitive neurons in the arcuate nuclei contribute to endogenous feeding rhythms

Ai-Jun Li, Michael F. Wiater, Marjolein T. Oostrom, Bethany R. Smith, Qing Wang, Thu T. Dinh, Brandon L. Roberts, Heiko T. Jansen, and Sue Ritter

Programs in Neuroscience, Washington State University, Pullman, Washington

Submitted 27 February 2012; accepted in final form 4 April 2012

Li AJ, Wiater MF, Oostrom MT, Smith BR, Wang Q, Dinh TT, Roberts BL, Jansen HT, Ritter S. Leptin-sensitive neurons in the arcuate nuclei contribute to endogenous feeding rhythms. *Am J Physiol Regul Integr Comp Physiol* 302: R1313–R1326, 2012. First published April 4, 2012; doi:10.1152/ajpregu.00086.2012.—Neural sites that interact with the suprachiasmatic nuclei (SCN) to generate rhythms of unrestricted feeding remain unknown. We used the targeted toxin, leptin conjugated to saporin (Lep-SAP), to examine the importance of leptin receptor-B (LepR-B)-expressing neurons in the arcuate nucleus (Arc) for generation of circadian feeding rhythms. Rats given Arc Lep-SAP injections were initially hyperphagic and rapidly became obese (the "dynamic phase" of weight gain). During this phase, Lep-SAP rats were arrhythmic under 12:12-h light-dark (LD) conditions, consuming 59% of their total daily intake during the daytime, compared with 36% in blank-SAP (B-SAP) controls. Lep-SAP rats were also arrhythmic in continuous dark (DD), while significant circadian feeding rhythms were detected in all B-SAP controls. Approximately 8 wk after injection, Lep-SAP rats remained obese but transitioned into a "static phase" of weight gain marked by attenuation of their hyperphagia and rate of weight gain. In this phase, Arc Lep-SAP rats exhibited circadian feeding rhythms under LD conditions, but were arrhythmic in continuous light (LL) and DD. Lep-SAP injections into the ventromedial hypothalamic nucleus did not cause hyperphagia, obesity, or arrhythmic feeding in either LD or DD. Electrolytic lesion of the SCN produced feeding arrhythmia in DD but not hyperphagia or obesity. Results suggest that both Arc Lep-SAP neurons and SCN are required for generation of feeding rhythms entrained to photic cues, while also revealing an essential role for the Arc in maintaining circadian rhythms of ad libitum feeding independent of light entrainment.

arcuate nucleus; circadian rhythms; obesity; hypothalamus

THE HYPOTHALAMUS PLAYS A KEY role in the generation and coordination of rhythms that sustain homeostasis. Lesion studies have repeatedly shown that destruction of the mediobasal hypothalamus (MBH), including the arcuate nucleus (Arc), disrupts the day/night distribution of feeding (12, 20, 39, 56, 57, 74), as well as causing obesity and hyperphagia (4, 11, 35). Furthermore, the Arc contains oscillators that maintain their intrinsic rhythms for several days in culture (1). The rhythms of some Arc oscillators are shifted in response to the anticipation of a restricted meal (54) or to fasting (32). Some are entrained to the photoperiod but, unlike those in the suprachiasmatic nucleus (SCN), exhibit peaks during the night (1). Thus, the Arc stands out as a critical nexus for signals governing food intake. Additionally, the Arc may play a role in the generation of feeding rhythms (14, 26, 77, 78) because it is reciprocally interconnected with the SCN (47, 59, 91), which is recognized as a key site for entrainment of circadian rhythms to the light-dark (LD) cycle (34). However, the role of the Arc in the generation of feeding rhythms remains to be clarified.

The Arc region plays a pivotal role in mediating effects of leptin, a fat-derived hormone with major effects on feeding and body weight. Leptin's actions are mediated by its effect on the leptin receptor B, LepR-B (28), which is densely expressed in the Arc on various cell types of known importance for food intake (6). Arc area lesions block major effects of exogenous leptin on food intake and body weight (13, 15, 21, 23). Furthermore, LepR-B has been implicated in the circadian control of feeding, as both *ob/ob* mice that lack leptin (99) and Zucker *fa/fa* rats that lack functional leptin receptors (96) have disrupted day-night feeding patterns (3, 27, 29, 36, 58, 82).

In the present experiments, we examined the role of LepR-B-expressing neurons in the Arc region on circadian ad libitum feeding rhythms. To destroy these neurons, the targeted toxin, saporin conjugated to leptin (Lep-SAP), was injected into the Arc. This conjugate binds to the leptin receptor, is internalized, and ultimately causes cell death by disrupting ribosomal function (93). We evaluated Lep-SAP effects on feeding rhythms under LD conditions and in continuous light (LL) and continuous dark (DD) conditions to more accurately define the role of the Arc in circadian feeding rhythms. We also compared Arc Lep-SAP lesions on feeding rhythms and body weight to a second group of rats receiving Lep-SAP injections into the ventromedial nucleus of the hypothalamus (VMN) and a third group of rats with electrolytic lesions of the SCN. The results reveal an important role for leptin-sensitive neurons in the Arc region in the production of feeding rhythms.

MATERIALS AND METHODS

Animals. Male Sprague-Dawley (S/D) (Simonsen Laboratories) and Zucker *fa/fa* fatty (Charles River Laboratories International) rats were housed individually in an animal care facility approved by the Association for Assessment and Accreditation of Laboratory Animal Care. Rats were maintained on a 12:12-h light (0700–1900)-dark cycle with ad libitum access to standard pelleted or powdered rodent diet (F6 Rodent diet; Harlan Teklad) and tap water, except as noted below. All experimental procedures were approved by Washington State University Institutional Animal Care and Use Committee, which conforms to National Institutes of Health Guidelines.

Injection of Lep-SAP and B-SAP into the arcuate nucleus. For stereotaxic microinjections, rats were anesthetized using 1.0 ml/kg body wt of a ketamine-xylazine-acepromazine cocktail in 0.9% saline solution (50 mg/kg ketamine HCl, Fort Dodge Animal Health; 5 mg/kg xylazine, Vedco; and 1 mg/kg acepromazine, Vedco). Appropriate dose and volume of Lep-SAP (Advanced Targeting Systems) were determined in preliminary studies. Injections were made into two sites, unilaterally or bilaterally, into each Arc. At doses equal to or less than 23.3 ng/injection site, Lep-SAP dissolved in 0.1 M PBS (pH 7.4)

Address for reprint requests and other correspondence: A.-J. Li, Dept. of Veterinary and Comparative Anatomy, Pharmacology, and Physiology, College of Veterinary Medicine, Washington State Univ., Pullman, WA 99164-6520 (e-mail: aijunli@vetmed.wsu.edu).

had only a weak lesioning effect on proopiomelanocortin (*Pomc*) or agouti gene-related peptide (*Agrp*) expression, producing less than 50% reduction of gene expression in the Arc. A dose of 56.5 ng Lep-SAP per injection site delivered bilaterally in a 50-nl volume at two loci in the Arc (i.e.., 226 ng/rat) produced an effective, localized, and reproducible lesion of the Arc with minimal damage to surrounding areas and was utilized for all Arc injections, except as noted. Controls were injected with an equivalent amount of blank-saporin (B-SAP; Advanced Targeting Systems), SAP conjugated to a peptide with no known receptor. Stereotaxic coordinates were as follows: for the rostral sites, 2.3 mm caudal and ± 0.45 mm lateral to bregma and 8.6 mm ventral to dura mater; and for the caudal sites, 3.3 mm caudal and ± 0.45 mm lateral to bregma and 8.8 mm ventral to dura mater (65). Injections were made with a Picospritzer (Parker) connected to a pulled glass capillary pipette (30-μm tip diameter). Fluid movement in the pipette was monitored microscopically. The solution was injected slowly over a 5-min period, and the pipette was removed slowly from the brain 5 min after the end of the injection.

Real-time PCR. For real-time PCR, rats were anesthetized deeply with isoflurane (Halocarbon Products) at the end of experimentation and killed by decapitation. The protocol used for PCR was modified from our previous report (51). After total RNA isolation from hypothalamic homogenates and reverse transcription, real-time PCR reaction was performed in triplicate using Platinum Taq DNA polymerase (Invitrogen), SYBR green I, with 5 μl of diluted cDNA in a final reaction volume of 25 μl. The amplification was followed by 40 cycles of denaturation at 94°C for 15 s, annealing at 58°C for 10–15 s and extension at 72°C for 15–20 s, with a CFX96 real-time system (Bio-Rad Laboratories). Finally, a melting curve was generated by stepwise increases in temperature (0.5°C increase every 10 s) for 80 cycles starting at 55°C. The threshold cycle (C_t) was determined with CFX manager software (Bio-Rad Laboratories). Gene expression was evaluated by means of a comparative C_t method and normalized to *β-Actin* expression. The primers used in the experiments for *Agrp* (GenBank accession no. AF206017) were 5′- gca gac cga gca gaa gat gt −3′ and 5′- gac tcg tgc agc ctt aca ca −3′; for *Pomc* (no. BC058443), 5′- ctc ctg ctt cag acc tcc at −3′ and 5′- ttt cag tca agg gct gtt ca −3′; and for *β- Actin* (no. BC063166), 5′- aga tta ctg ccc tgg ctc ct −3′ and 5′-aca tct gct gga agg tgg ac −3′. The dissociation curves of each primer pair used in the present study showed a single peak, and the samples tested after the PCR reactions had a single expected DNA band on agarose gels.

Immunohistochemistry. For experiments in which immunohistochemistry (IHC) was used for lesion analysis, rats were killed at the end of experimentation by deep isoflurane anesthesia. After perfusion and fixation in 4% formalin in PBS, brains were sectioned coronally into serial sets (30 or 40 μm thickness) and stained using standard avidin-biotin-peroxidase or immunofluorescent IHC technique (13, 52). The following primary antibodies were used: goat anti-AGRP (1:1,000; Neuromics), sheep anti-alpha-melanocyte stimulating hormone (α-MSH) (1:10,000; Millipore), rabbit antisteroidogenic factor-1 (SF-1) was (1:1,000; Millipore), rabbit anti-arginine vasopressin (AVP) (1:15,000; Millipore), and goat anti-SAP (1:1,000; Advanced Targeting Systems) antibodies.

In the absence of a leptin receptor antibody that was reliable in our hands, α-MSH- and AGRP-positive cells, both present in the Arc and known to express the LepR-B receptor, were used to assess the effectiveness of Arc-directed injections on the targeted neurons. Immunoreactive neurons were counted in three consecutive coronal sections at each of four anatomical levels. The presence of SF-1 was evaluated to assess the effect of the VMN-directed lesion. SF-1 is expressed in nuclei of VMN neurons that coexpress LepR-B (22), making them a potentially useful indicator of lesion localization. AVP is expressed in the SCN and was used to assess the effect of Arc-directed lesion on SCN area. The distribution of the SAP conjugates surrounding the injection sites was estimated in a subset of rats using anti-SAP antibody to detect the SAP moiety in cells and extracellular fluid 4 h after Arc-targeted Lep-SAP and B-SAP injections.

Selectivity of Lep-SAP for lesioning LepR-B-expressing neurons. Lep-SAP was injected into Zucker *fa/fa* rats, which lack functional leptin receptors. To determine the specificity of the Lep-SAP lesion for neurons expressing leptin receptors, Lep-SAP or B-SAP was injected unilaterally into the Arc of anesthetized Zucker *fa/fa* fatty rats and S/D controls using the parameters as described above. Zucker *fa/fa* fatty rats express a mutation on the extracellular domain of their leptin receptors (16, 66) that reduces the affinity of the receptors for leptin (19). Hypothalamic tissue was collected 3 wk later and processed for immunohistochemical detection of α-MSH and AGRP using standard IHC techniques as described above.

Effect of Lep-SAP on leptin responsiveness. Rats were injected into the Arc with Lep-SAP or B-SAP, as described above, to assess the lesion effects on responsiveness to exogenous leptin. Three weeks later, they were anesthetized and implanted stereotaxically with a 26-gauge stainless-steel cannula into the lateral ventricle (LV) using the following coordinates: 1.0 mm caudal to bregma, 1.5 mm lateral to midline and 3.9 mm ventral to the skull surface (65). After 1 wk of recovery, their responsiveness to LV administration of leptin or artificial cerebrospinal fluid (aCSF) was tested. Recombinant mouse leptin (2.5 μg/3 μl; EMD Chemicals) in aCSF or 3 μl of aCSF was delivered into the LV over a 3-min period using a PB-600 repeating dispenser (Hamilton). Injections were made daily for three consecutive days. Daily food intake and body weight were measured beginning prior to and continuing throughout the 3-day injection period.

Feeding and metabolic rhythms during the dynamic phase of the Arc-directed Lep-SAP lesion. Feeding and metabolic parameters were evaluated between 1 and 8 wk after Arc injections of Lep-SAP or B-SAP using open-circuit Oxymax chambers (Columbus Instruments). Rats were singly housed in the chambers, which were maintained at 23–24°C on a LD cycle in which lights were on from 0700 to 1900. Powdered F6 rodent food (Teklad) and water were available ad libitum when rats were in the chambers, except as noted. Rats were acclimatized to the monitoring cages for 2 days prior to the beginning of automated data collection. Feeding data were collected each minute using the CLAX system (Columbus Instruments). Food consumed was double-plotted in 30-min bins in actogram format (i.e., as "eatograms"), using Clocklab software (Actimetrics). We use the term "eatogram" rather than "actogram" because this term conveys the important point that food intake, rather than food-related activity, was the measured variable in our studies. Double-raster plotted eatograms were generated as percentile distributions, with each nonzero count assigned one of five quantiles, according to the range of the total counts in each set. Lomb-Scargle periodograms were used to identify significant periodicities in the feeding data (67). The batch function, in which all data for each group are averaged into a single plot, was used to examine rhythmic tendencies in eatograms and periodograms. Batched analyses are valuable in showing and quantifying strong synchronous rhythms within a group. However, batch analyses also can be misleading because they may obscure individual rhythms that are asynchronous across the group. Therefore, we analyzed and reported both batch and individual data from our experiments. While in the Oxymax chambers, O_2 consumed ($\dot{V}O_2$) and CO_2 generated ($\dot{V}CO_2$) was measured for each rat by open circuit indirect calorimetry every 20 min. Then, respiratory exchange ratio (RER; the ratio of $\dot{V}CO_2$ over $\dot{V}O_2$, also known as the respiratory quotient, or RQ), was calculated. Metabolic rate (heat production or energy expenditure) was calculated by Oxymax as metabolic heat = (3.815 + 1.232 × RER) × $\dot{V}O_2$. After normalization with respect to body weight, averages of each parameter over 12 days for the diurnal and nocturnal periods, respectively, were calculated and compared. Locomotor activity in the *x*- and *z*-axes using infrared beam-breaks was also recorded and analyzed. Metabolic and activity data were analyzed using ClockLab software to produce batched and individual Lomb-

Scargle periodograms and to determine the presence of significant rhythms within the circadian range (20–28 h).

Feeding rhythms in the static phase in rats with Arc-directed injections of Lep-SAP. Rats used for dynamic-phase experiments described above were studied again during their static phase between 9 and 25 wk after Arc injections when hyperphagia was diminished and the rate of body weight gain was similar to controls. For static phase measurements, the B-SAP and Lep-SAP rats were housed in BioDAQ (Research Diets) computerized cages for automated meal monitoring. The timing and duration of feeding bouts were determined over a 54-day period and binomial data strings for each minute (yes or no for eating) were obtained. Feeding behavior was monitored in this way during LD (LD1; 3 days), DD (28 days), another LD (LD2; 7 days), and LL (16 days) conditions. The experimental room was entered for animal maintenance only on an intentionally irregular schedule. Lesioned and control groups were tested together under each lighting condition. Analysis of meal monitor data was accomplished with ClockLab software as above.

Injections of Lep-SAP and B-SAP into the VMN. To help localize the lesion effects produced by the Arc-directed Lep-SAP injections, we also injected Lep-SAP and B-SAP bilaterally into the adjacent VMN (100 nl/side or 226 ng/rat) in a separate group of rats. Stereotaxic coordinates were as follows: 2.9 mm caudal and ± 0.75 mm lateral to bregma and 8.0 mm ventral to dura mater (65). Food intake and body weight were measured beginning immediately after surgery. Feeding rhythms were tested in rats with VMN injections of B-SAP and Lep-SAP beginning 7 wk after injections using the BioDAQ automatic meal monitoring chambers, as described above. This measurement time was chosen to approximate the start of the static phase in the Arc-injected Lep-SAP group. Food intakes were analyzed using ClockLab software during LD and DD conditions. Lesions were analyzed using immunohistochemical detection of α-MSH and SF-1,

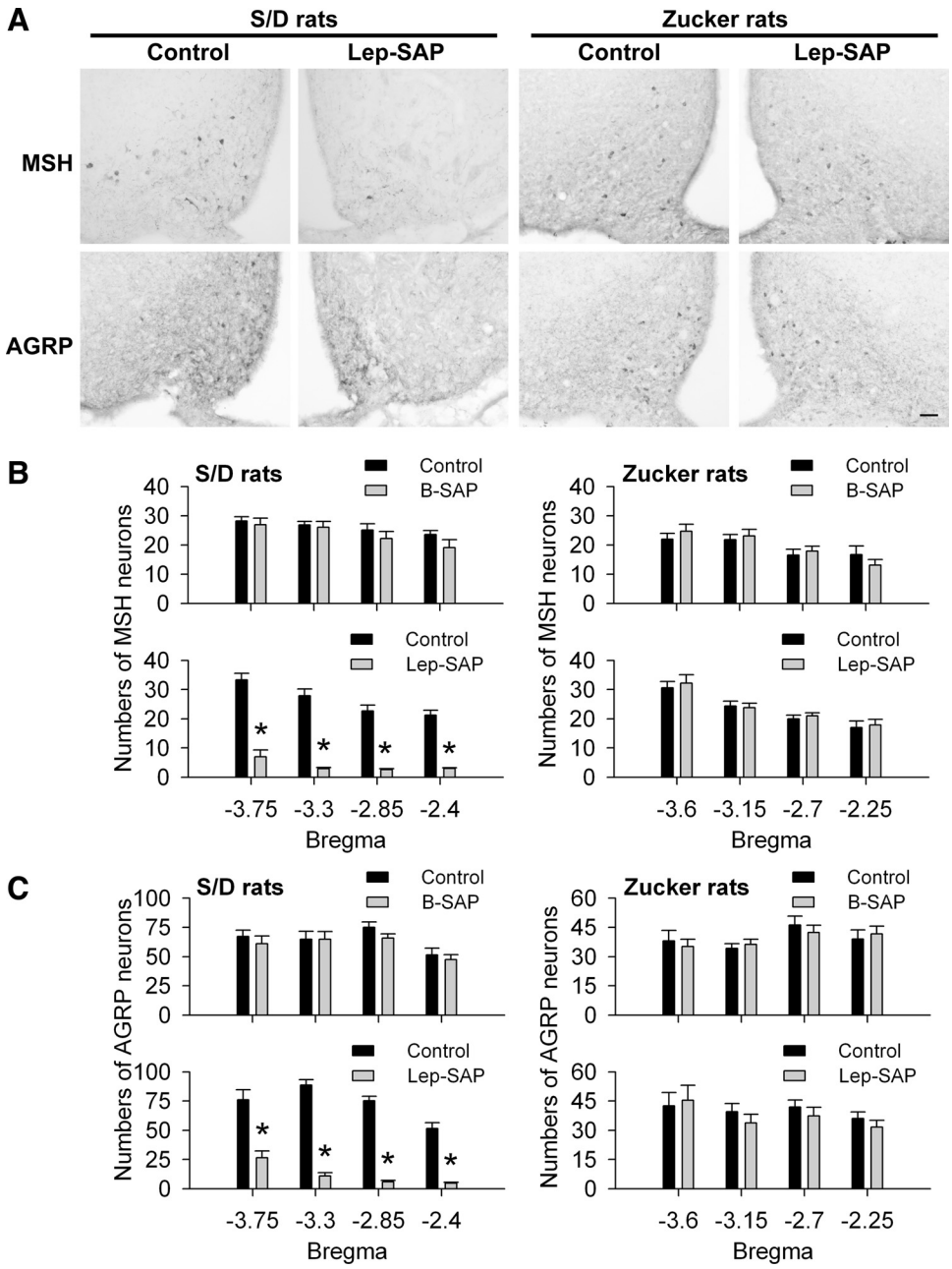

Fig. 1. Leptin receptor-dependent lesion of arcuate nucleus (Arc) neurons by unilateral leptin conjugated to saporin (Lep-SAP) injection. *A*: representative immunohistochemical (IHC) images of alpha-melanocyte stimulating hormone (α-MSH) and agouti gene-related peptide (AGRP) neurons after unilateral injection of Lep-SAP into the Arc in Sprague-Dawley (S/D) or Zucker *fa/fa* (Zucker) rats. Calibration bar = 100 μm. Numbers of α-MSH-positive (*B*) and AGRP-positive (*C*) cell bodies in the Arc of S/D or Zucker *fa/fa* rats (n = 3 or 4 rats per group) after unilateral injection of Lep-SAP or control blank saporin (B-SAP). Quantified data are shown for four hypothalamic levels, each indicated in millimeters caudal to bregma. *P < 0.001 vs. the noninjected (contralateral) side.

which are expressed in neurons possessing LepR-B (22), to assess the integrity of the Arc and VMN, respectively. Note that in this paper, we distinguish between the ventromedial nucleus of the hypothalamus (VMN), a specific hypothalamic nucleus, and the ventromedial hypothalamus (VMH), which is less specific and generally encompasses an area in the medial basal hypothalamus that includes the Arc. However, when referring to published work in which the authors use the term VMH, we also use that term.

Electrolytic lesions of the SCN. For comparison with Arc-directed Lep-SAP lesions, we also examined the effects of SCN lesion on food intake, feeding rhythms, and body weight. Because the neurochemical phenotypes of leptin-sensitive SCN neurons are still unclear, effects of Lep-SAP on SCN neurons would be difficult to establish. Therefore, we utilized electrolytic lesions in this experiment. Rats were anesthetized with 1 ml/kg of Xyket (xylazine, 13 mg/kg + ketamine 87 mg/kg ip) and electrolytic SCN lesions (SCNX), or sham lesions were produced, as described previously (38). Radiotransmitters (E4000, MiniMitter) were implanted at the time of SCN surgery. Body temperature and activity data were recorded continuously in 1-min epochs with the aid of a receiver (RTA 500, MiniMitter). Behavioral assessment of lesion completeness began 2 wk after surgery. Only those SCNX rats that exhibited a loss of both body temperature and activity rhythms following surgery were included in the study. Feeding studies and analyses were then performed as described above for Lep-SAP rats.

Statistical analysis. For standard statistical comparisons between Lep-SAP and B-SAP rats, unpaired Student's *t*-tests, one-way, two-way, or repeated-measure ANOVA was used as appropriate. Multiple comparisons between individual groups were tested using a post hoc Fisher's paired least significant difference test. Differences were considered significant if $P < 0.05$. Results are presented as means ± SE.

RESULTS

Selectivity of Lep-SAP in lesioning LepR-B-expressing neurons. Figure 1 shows the results of unilateral injections of Lep-SAP or B-SAP were made into the Arc of Zucker *fa/fa* fatty rats or into the Arc of S/D rats. In S/D rats, the numbers of α-MSH- and AGRP-positive cells were significantly decreased in the Arc on the side injected with Lep-SAP compared with the noninjected side. Overall, numbers of α-MSH- or AGRP-positive cells in the Arc (between −3.75 to −2.4 mm caudal to bregma) were decreased to 18.2% and 16.4%, respectively, of the number on the noninjected side. In contrast to S/D rats, unilateral injection of Lep-SAP into the Arc in Zucker *fa/fa* rats did not reduce the number of either α-MSH- or AGRP-positive cell bodies on the injected side, compared with the noninjected side. There were no significant changes in the number of α-MSH- or AGRP-expressing cell bodies in the Arc of B-SAP-injected controls. These results indicate that Lep-SAP toxicity is dependent on its internalization with the LepR-B receptor.

Arc Lep-SAP injections impaired feeding and body weight responses to leptin. Lateral ventricular leptin injections in B-SAP rats significantly decreased 24-h food intake on *days 1–3* and body weight on *days 2* and *3* after the injection ($P < 0.01$), but they had no effect on feeding or body weight in Lep-SAP rats during the 3-day test period (Fig. 2, *A* and *B*). Results suggest that the toxin destroyed leptin-responsive Arc neurons crucial for control of feeding and body weight by leptin.

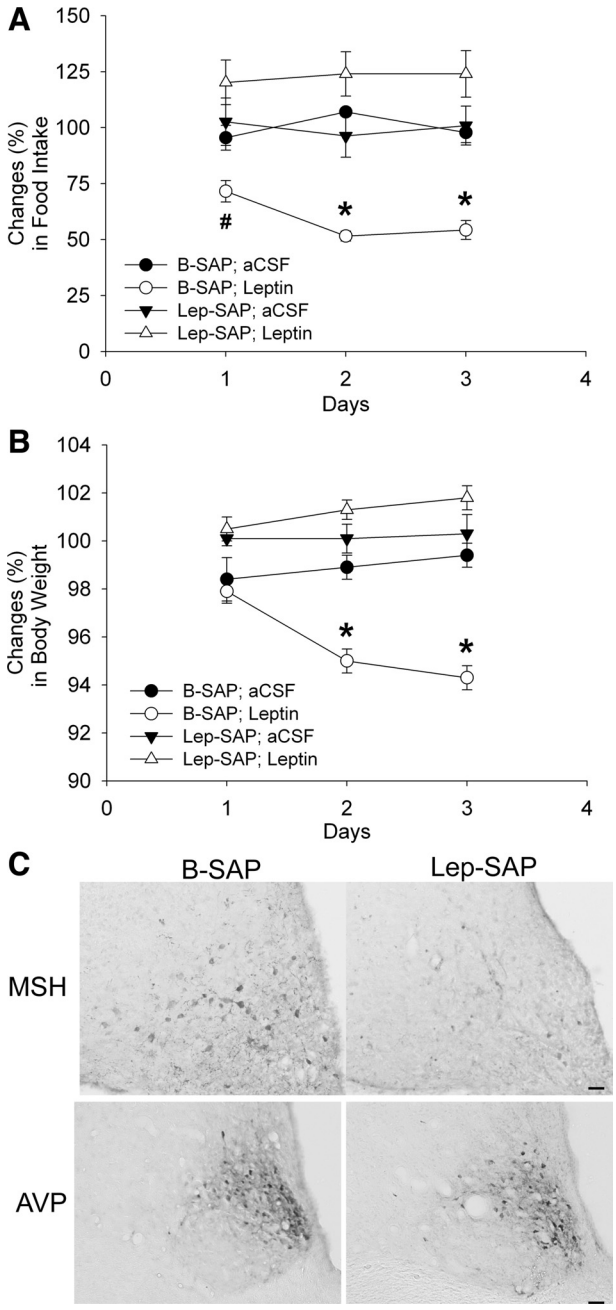

Fig. 2. Effects of Arc injections of Lep-SAP and B-SAP on feeding and body weight changes in response to leptin and on Arc α-MSH and suprachiasmatic nuclei (SCN) AVP immunohistochemistry. *A*: food intake, expressed as a percentage of intake on the baseline day (1 day prior to the start of leptin or aCSF injections). *B*: body weight on *days 1*, *2*, and *3* (as a percentage of body weight on the baseline day) of daily lateral ventricular leptin (2.5 μg in 3.0 μl) or artificial cerebrospinal fluid (aCSF; 3 μl) injections ($n = 6–8$ rats per group). #$P < 0.01$; *$P < 0.001$ vs. B-SAP rats. *C*: coronal sections through basal hypothalamus. Top row shows α-MSH-immunoreactivity in the Arc (2.8 to 3.0 mm caudal to bregma) of a rat injected with B-SAP (*left*) or Lep-SAP (*right*). Bottom row shows arginine vasopressin (AVP)-immunoreactivity in the SCN (0.6 to 0.7 mm caudal to bregma) of rats injected into the Arc with B-SAP (*left*) or Lep-SAP (*right*). Calibration bar = 20 μm, or 40 μm for AVP, α-MSH, respectively.

Effects of arc Lep-SAP injections on immunohistochemical markers and gene expression. Figure 2*C* shows effects of bilateral Arc injection of Lep-SAP on Arc α-MSH and SCN AVP neurons. Between 2.3 and 3.6 mm caudal to bregma, the

number of Arc α-MSH neurons was reduced from an average of 34.4 ± 0.9 cells/section/side in B-SAP rats ($n = 7$) to 7.2 ± 0.8 cells/section/side in Lep-SAP rats ($n = 7$; $P < 0.001$), indicating that Lep-SAP damaged Arc neurons that express leptin receptors. The figure also shows AVP-immunoreactivity in the SCN. The normal appearance and integrity of the tissue suggest that the SCN remains intact in the Lep-SAP rats.

Immunofluorescent detection of internalized SAP using anti-SAP antibody reveals an approximation of the diffusion of the conjugate from the injections site. As can be seen in Fig. 3, the internalization appears to be limited to a relatively small sphere at the microinjector tip and along its tract, where neuron uptake is nonspecific due to damage. However, it should be noted that this approach undoubtedly underestimates the loss of neurons resulting from the Lep-SAP injection. This is primarily because the small number of internalized SAP molecules sufficient to cause cell death may fall below the detection limit of the immunohistochemical technique.

Using RT-PCR for genes encoding neuropeptides coexpressed with LepB-R, we found that *Agrp* and *Pomc* expression was reduced in the hypothalamus in rats injected with Lep-SAP: *Agrp* mRNA was reduced to 11.4 ± 1.6% of B-SAP control levels, and *Pomc* mRNA was reduced 21.4 ± 2.9% of control ($P < 0.001$; $n = 5$ or 6 rats). In addition, a stronger negative correlation between gene expression in the hypothalamus and food intake or body weight gain was observed for Lep-SAP rats compared with B-SAP rats (data not shown).

Feeding and metabolic rhythms during the dynamic phase of the Arc-directed Lep-SAP lesion. All Arc Lep-SAP rats were hyperphagic and gained weight rapidly during the 8 wk following injections (Fig. 4*A*). At the beginning of *week 2*, the average 24-h food intake was 23.4 ± 0.8 g for B-SAP rats ($n = 7$), which was significantly less ($P < 0.001$) than the average of 45.9 ± 1.7 g in Lep-SAP rats ($n = 7$). Light period intake as a percentage of 24-h food intake was 35.5 ± 3.8% and 58.6 ± 4.1% for B-SAP and Lep-SAP rats, respectively, during the early dynamic phase. The Lep-SAP hyperphagia gradually attenuated during the dynamic phase, but food intake remained significantly greater than in B-SAPs. At *week 8*, 24-h food intake was 26.1 ± 0.9 g in B-SAPs and 36.1 ± 5.0 g in Lep-SAP rats. The percentage of daytime food intake was 18.1% and 31.4% for B-SAP and Lep-SAP rats, respectively.

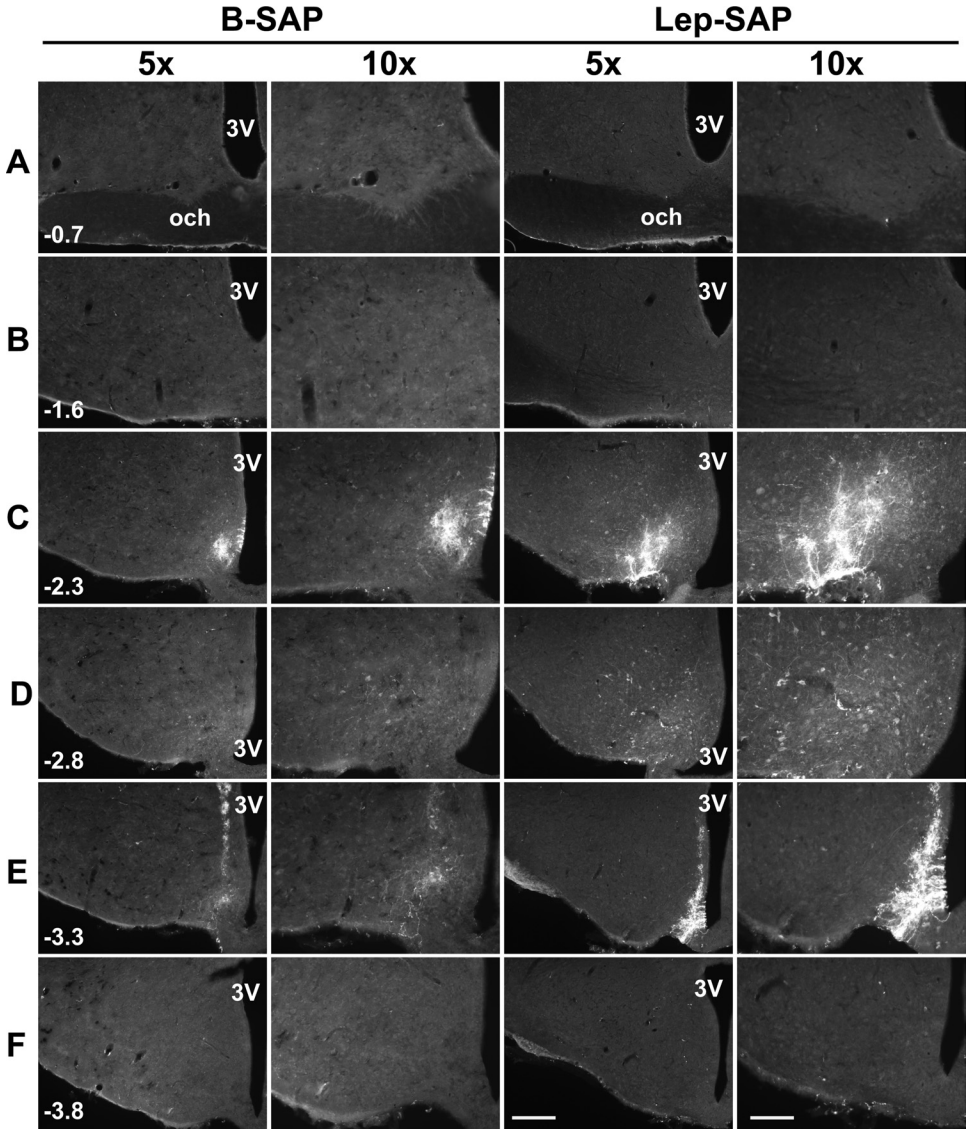

Fig. 3. Distribution of SAP-immunoreactivity after injection of B-SAP or Lep-SAP into the Arc. Injections (50 nl each) were made at two rostrocaudal levels in the Arc (−2.3 and −3.3 mm, caudal to bregma). Rats were euthanized 4 h later. Distribution of SAP immunoreactivity was shown at two magnifications (×5 and ×10) at each of six rostrocaudal levels for a representative rat from each group between SCN (*A*) and the mammillary recess of the third ventricle (*F*) (distances in millimeters, caudal to bregma, are shown in the first image for each level). Immunofluorescent images were overexposed to show the anatomic structures. Calibration bar = 200 μm, 400 μm for ×5 and ×10, respectively. 3V, third ventricle; och, optic chiasm.

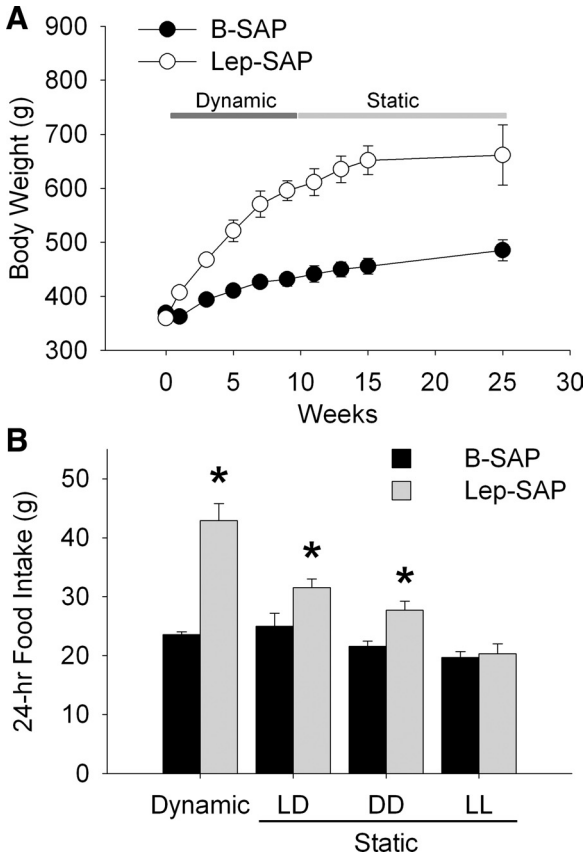

Fig. 4. Body weight and food intake during the dynamic and static phases of weight gain in rats injected into the Arc with B-SAP or Lep-SAP. *A*: body weight (g) for the two groups. In the Lep-SAP group, the dynamic phase of extreme hyperphagia and rapid weight gain, lasting about 8 wk, was followed by the static phase of attenuated rate of weight gain and attenuated hyperphagia. *B*: average daily food intake across all days in the dynamic and during different lighting conditions in static phases for the Lep-SAPs ($n = 7$) and B-SAPs ($n = 6$). In the static phase, total daily food intake is shown for three different light conditions: 12:12-h light-dark (LD), continuous dark (DD), and continuous light (LL). *$P < 0.05$, Lep-SAP rats vs. B-SAP rats in each lighting condition.

Lep-SAP rats gained weight rapidly during the dynamic phase (Fig. 4*B*). Body weight was significantly increased at all time points after the injection of Lep-SAP beginning on *day 3* ($P < 0.001$). Four weeks postinjection, the mean body weight of B-SAP controls increased by 21.8 g or 5.9%, while the mean body weight of Lep-SAP rats increased by 140.7 g or 39.1%. The mean body weight gain per week over the 8 wk of the dynamic phase was 6.7 ± 1.0 g for B-SAP rats and 24.4 ± 2.0 g for Lep-SAP rats.

Figure 5 shows eatograms and Lomb-Scargle periodograms for B-SAP and Lep-SAP rats during the dynamic phase under LD and DD conditions over a 25-day period. B-SAP rats had rhythmic feeding in both LD and DD. In contrast, no individual Lep-SAP rat had a significant circadian rhythm in LD, but the batch analysis yielded a very weak rhythm. Since it is unlikely that rats that were arrhythmic in LD would be rhythmic in DD, only half of each group ($n = 3$ or 4 for B-SAP and Lep-SAP rats, respectively) was tested during DD in the dynamic phase. Unlike B-SAP rats, which displayed a free-running rhythm in DD, no individual Lep-SAP or batched Lep-SAP periodogram was rhythmic in DD.

Respiratory exchange ratio (or "respiratory quotient") and metabolic rate were also measured during the dynamic phase. RER was consistently elevated in Lep-SAP rats, compared with controls, indicating a higher level of carbohydrate metabolism in the lesioned rats and consistent with the lipogenesis and obesification that was apparent in these rats. When plotted in actogram format and subjected to Lomb-Scargle analysis, the RER was found to be rhythmic in B-SAP rats with a period of 23.7 ± 0.2 h but was arrhythmic in Lep-SAP rats during LD and remained so during DD. RER results are consistent with the circadian distribution of feeding and fasting in B-SAPs, associated with increased fat metabolism and lower RER during the fasting state than in the postingestive state, and with the absence of circadian feeding rhythms in the Lep-SAP group. In contrast, the continuously feeding (arrhythmic) Lep-SAP rats had higher RER values (>1.0) throughout the circadian cycle, consistent with their persistent postingestive state, high carbohydrate diet of rat chow and body weight gain (33, 46, 49, 50, 79, 83, 85). Overall, the RER was 0.903 ± 0.005 for B-SAP rats during the day and 0.929 ± 0.005 during the night ($P < 0.001$). For Lep-SAP rats, RER was 1.083 ± 0.006 during the day and 1.086 ± 0.004 during the night ($P > 0.6$).

In contrast to RER, in LD metabolic rate ($kcal \cdot kg^{-1} \cdot h^{-1}$) was rhythmic for both B-SAP rats (4.55 ± 0.11 for day vs. 6.32 ± 0.18 for night; $P < 0.001$) and Lep-SAP rats (4.38 ± 0.22 for day vs. 5.37 ± 0.28 for night; $P < 0.01$) with a peak during the dark phase. Lep-SAP rats were arrhythmic for metabolic rate in DD. Batched Lomb-Scargle periodograms (not shown) revealed a rhythm with a period of 24.0 h for both groups in LD, but only for B-SAP rats in DD with a tau of 24.2 h. Activity in the *x*- and *z*-axes was dampened in the Lep-SAPs, compared with controls but was still significantly greater during the dark period than during the light period. The reduced level of Lep-SAP activity in the dynamic phase may have been due, in part, to space limitation in the metabolic cages as the lesioned rats became progressively obese. Horizontal (*x*) activity (in counts/20 min) in B-SAP and Lep-SAP rats was 72.3 ± 6.2 in day vs. 241.5 ± 17.9 in night ($P < 0.001$), and 85.0 ± 6.2 in day vs. 112.4 ± 12.5 in night ($P < 0.05$), respectively. Vertical (*z*) activity (in counts/20 min) in B-SAP and Lep-SAP rats was 32.8 ± 3.6 in day vs. 163.4 ± 11.2 in night ($P < 0.001$), and 34.6 ± 5.8 in day vs. 53.1 ± 5.8 in night, respectively ($P < 0.05$).

Feeding rhythms during the static phase of the Arc Lep-SAP lesion. Table 1 provides quantitative data showing circadian period lengths and robustness of the rhythms of food intake under the different photic conditions for each group. The robustness (or consistency) of the rhythm across time, also referred to as rhythm stationarity, is indicated by the amplitude of the periodogram. Also shown is a "masking score," calculated as the percent of daily feeding that occurred during light (or subjective light for DD and LL) divided by total 24-h food intake. Food intake was decreased in Lep-SAP rats during the static phase compared with their intake during the dynamic phase (Fig. 4; Table 1). During the static phase, the 3-day daily average intake in LD was 25.0 ± 2.2 g and 31.6 ± 1.5 g for B-SAPs ($n = 6$) and Lep-SAPs ($n = 7$), respectively. The amount gained per week in the static phase was 5.0 ± 2.2 g for B-SAP rats and 13.0 ± 5.0 g for Lep-SAP rats. Thus, the Lep-SAP rats remained obese and hyperphagic, but their food

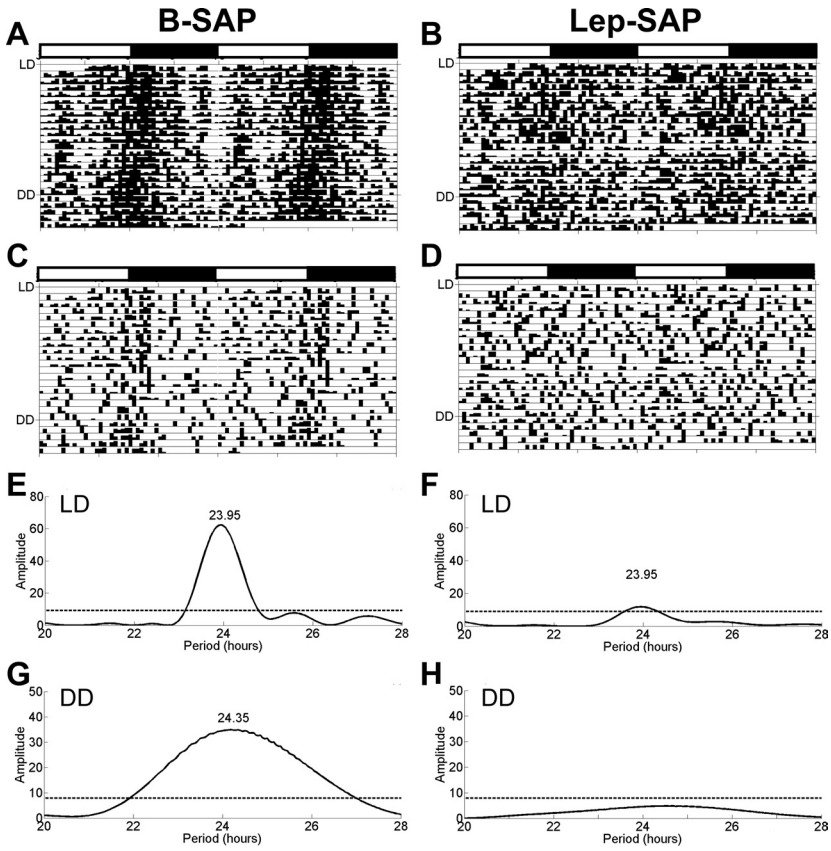

Fig. 5. Double raster plots for feeding (eatograms) and Lomb-Scargle periodograms for feeding rhythm analysis during the dynamic phase in B-SAP or Lep-SAP rats. Each eatogram was plotted with a 30-min block size using ClockLab. *A* and *B*: batched eatograms for the respective groups. *C* and *D*: individual eatograms for representative rats from each group. *A–D*: plots show eating under two conditions: 12:12-h LD for 20 days and DD for 5 days. White and black bars above eatogram plots indicate light and dark periods during LD, respectively. Periodograms of feeding rhythms of B-SAP group (*E*) and Lep-SAP group (*F*) under LD conditions. Periodograms of feeding rhythms of B-SAP group (*G*) and Lep-SAP group (*H*) under DD conditions. The dotted line represents the amplitude of the periodogram required for significance ($P < 0.05$). The numbers associated with the peaks in periodograms are tau (in hours).

intake and rate of body weight gain were much attenuated during the static phase compared with the dynamic phase.

Static phase food intake was significantly greater in Lep-SAP than in B-SAP rats in both LD and DD ($P < 0.05$), primarily during the light or subjective light period (Table 1). In contrast, total daily intake during LL was significantly less in both groups than during either LD or DD ($P < 0.05$) and did not differ between groups (Fig. 4*B*). Figure 6, *A–D* shows the batched and representative individual eatograms of feeding collected over 54 days during LD, DD, a second LD, and LL conditions. By batch analysis, both groups were rhythmic during the second 7-day LD conditions. However, this rhythm in the Lep-SAP group was expressed by only three of the seven lesioned rats. The remaining four lesioned rats were arrhythmic during LD (Table 1). Figure 6, *E–J* shows batched Lomb-Scargle periodograms for food intake during DD, second LD, and LL. B-SAP rats had a rhythm of 24.4 h during DD and 25.4 h during LL. Over the entire 4 wk of DD, B-SAP rats exhibited a synchronous free-running feeding rhythm. In LL, 2 of the 6 B-SAP rats became arrhythmic. In contrast, only 2 of the 7 Lep-SAP rats were very weakly rhythmic during DD, and none were rhythmic in LL. In addition, Lep-SAP rats were collectively arrhythmic under both LD and DD conditions when analyzed by batched periodogram. Furthermore, no free-running rhythm was exhibited by Lep-SAP rats, individually or collectively, by eatogram analysis during either LL or DD. Absence of an entrained rhythm in Lep-SAPs is apparent in the distribution of feeding during the first 2 days of DD, when 42.3 ± 2.6% of total 24-h intake in Lep-SAPs was consumed during the subjective light period, compared with 22.6 + 2.1% in the B-SAPS. During the 7 days of the second LD period following DD, B-SAP and L-SAP rats ate 25.1 ± 4.4% and 25.2 ± 3.1% of total 24-h intake during the light period, respectively. This suggests that the apparent rhythm of feeding behavior of Lep-SAP rats during LD was controlled by photic cues and not derived from feeding cues.

Feeding rhythms and body weight in rats after injection of Lep-SAP into the VMN. In contrast to Arc Lep-SAP rats, rats with VMN Lep-SAP did not become hyperphagic or obese (Fig. 7, *A* and *B*). Indeed, total daily food intake tended to be less in VMN Lep-SAP rats ($n = 7$) than in VMN B-SAP rats ($n = 6$). Although body weights at the time of the injections did not differ between groups, VMN Lep-SAP rats weighed less at the end of the experiment than B-SAP rats (367.0 ± 7.8 g and 386.0 ± 5.3 g, respectively, $P < 0.05$).

Batched and representative individual eatograms for VMN B-SAP and Lep-SAP rats (Fig. 8) revealed rhythmic feeding in LD and free-running rhythms during DD. Batched Lomb-Scargle periodograms show these to be significant circadian rhythms with similar periods. Using peak amplitude as an estimate of rhythm robustness, we found no significant difference between the VMN B-SAP and VMN Lep-SAP groups ($P > 0.3$). None of the VMN Lep-SAP rats became arrhythmic for feeding.

IHC results revealed that SF-1-positive neurons were reduced in the VMN, but α-MSH-positive neurons were still present in the Arc of VMN injected Lep-SAP rats (Fig. 7*C*). These results indicate Lep-SAP injections into the VMN, using the same dose and volume as for the Arc, damaged LepR-B

Table 1. *Analysis of feeding rhythms*

	Late Dynamic	Static			
Phase	LD (4 days)	LD 1 (3 days)	DD (28 days)	LD 2 (7 days)	LL (16 days)
Rhythms					
Period, h					
B-SAP			24.4 ± 0.03	24.8 ± 0.3	25.5 ± 0.3
Lep-SAP			22.4 ± 0.9$	24.1 ± 0.2 $	ND
Amplitude (Robustness)					
B-SAP			45.2 ± 7.0	20.0 ± 2.6	10.5 ± 0.5
Lep-SAP			16.0 ± 3.0 $	26.0 ± 7.0 $	ND
% of Rhythmic rats					
B-SAP			100	100	67
Lep-SAP			29	43	0
Food Intake					
24-h, g					
B-SAP	26.1 ± 0.9	25.0 ± 2.2	26.2 ± 0.8	21.0 ± 1.3#	20.6 ± 3.1#
Lep-SAP	36.1 ± 5.9*#	31.6 ± 1.5*	37.4 ± 2.8*#	26.3 ± 1.9*#	23.5 ± 3.6#
12-h in Light, g					
B-SAP	4.8 ± 1.0	4.4 ± 0.9	6.0 ± 0.7	5.3 ± 1.0	6.9 ± 1.4#
Lep-SAP	12.4 ± 3.3*	10.5 ± 1.3*	16.1 ± 1.8*#	6.7 ± 1.0#	8.4 ± 1.4
12-h in Dark, g					
B-SAP	21.3 ± 0.9	20.6 ± 1.5	20.2 ± 0.5	15.7 ± 0.9#	13.7 ± 1.8#
Lep-SAP	23.7 ± 2.7	21.1 ± 0.9	21.3 ± 1.3	19.6 ± 1.0*	15.1 ± 2.4#
12-h in Light/24-h, %					
B-SAP	18.4 ± 3.4	16.7 ± 2.7	22.6 ± 2.1#	25.1 ± 4.4#	32.4 ± 3.5#
Lep-SAP	31.4 ± 4.7*	32.8 ± 3.1*	42.3 ± 2.6*#	25.2 ± 3.1#	36.3 ± 2.5

Feeding rhythm analyses and food intake during the late dynamic phase (4 days) and the four stages of the static phase: 3 days of 12:12-h light-dark (LD1) cycle, 28 days of continuous dark (DD), 7 days of second LD (LD2), and then 16 days of continuous light (LL). For feeding rhythm analysis, only the individual rats rhythmic by Lomb-Scargle periodogram were used to calculate the averages of period and amplitude (robustness). Because of the free run during DD and LL, only the first 2 days of food intakes of those stages are presented in order to evaluate the transitions between stages for subjective light or subjective dark. Note that for LD2, the period is not 24 h because rats were transitioning from DD during the 7 days. *Significant difference using a *t*-test ($P < 0.05$) between paired data for B-SAP and Lep-SAP rats. #Significant difference ($P < 0.05$) between LD1 values at the beginning of the static phase and another value in a different lighting condition of the same group. ND, no individual rat was found to be rhythmic. $Sample size for Lep-SAP rats was too small for statistical comparison.

neurons in the VMN but did not produce significant damage to Arc LepR-B neurons.

Effects of SCN lesion on body weight and feeding rhythms. The body weights at the time of surgery were 386.5 ± 1.0 g for sham rats ($n = 6$) and 383.4 ± 1.6 g for SCNX rats ($n = 7$; $P > 0.1$). Approximately 12 mo later, these rats were placed in the BioDAQ chambers for assessment of feeding rhythms, at which time, their body weights were 461.5 ± 13.1 g and 412.0 ± 11.5 g for sham and SCNX rats, respectively ($P < 0.05$). Feeding rhythms were measured for 25 days in LD and then 5 days in DD (Fig. 9). During LD, mean 24-h food intake was 26.1 ± 0.9 g and 25.6 ± 1.9 g, for sham and SCNX rats ($P > 0.8$), respectively. During DD, mean 24-h food intake was 27.5 ± 0.9 g and 24.5 ± 1.0 g for sham and SCNX rats ($P = 0.06$). Although total daily intake during LD and DD was similar for both groups, distribution across light and dark period differed significantly. During LD light period, mean food intake was 15.7% of total in shams and 41.0% of total for SCNX rats. During DD, the subjective light period mean food intake was 27.3% of total daily intake in sham rats and 50.6% of total in SCNX rats. Feeding in shams was rhythmic in both LD and DD, with a period length of 24.0 ± 0.03 h in LD and 24.3 ± 0.1 h during DD (Fig. 9). During LD, SCNX rats had a weak rhythm with a period length of 24.0 ± 0.1 h, but all were arrhythmic during DD.

DISCUSSION

As described previously for electrolytic lesions of the MBH (12, 43), Arc Lep-SAP lesions produced dynamic and subsequent static phases of feeding and weight gain. During the dynamic phase, lesioned rats were hyperphagic and gained weight rapidly. During the second week after the lesion Lep-SAP daytime intake was 59% of their total daily intake, compared with 36% in B-SAP rats. Dynamic phase feeding, as well as RER and metabolic rate, were arrhythmic in Lep-SAP rats under all lighting conditions. In contrast, significant feeding, RER, and metabolic rhythms were detected in all B-SAP controls during both LD and DD. Metabolic rate and RER have been shown to be rhythmic in controls during LD (69, 90), but they have not been examined previously in DD.

During the static phase of the Arc Lep-SAP lesion, hyperphagia and body weight gain were attenuated. All B-SAP rats and three of the seven Lep-SAP rats exhibited feeding rhythms that were in the circadian range and predominantly nocturnal during LD. However, feeding in DD was arrhythmic in Lep-SAPs, while retaining the expected free-running circadian periodicity in B-SAP rats. This persisting free-running rhythm in B-SAP rats with a tau in the circadian range in the absence of photic cues is a defining feature of an endogenous circadian rhythm generator, suggesting here that such a mechanism determines ad libitum feeding patterns and requires the Arc.

All Lep-SAP and two B-SAP rats became arrhythmic in LL. The loss of rhythmicity in intact rats in LL has been described previously (24). Thus, the loss of feeding rhythms and declines in total daily food intake in some control rats is not surprising. Arrhythmic Lep-SAP rats also showed a decrease in total daily food intake in LL, suggesting that photic information remains

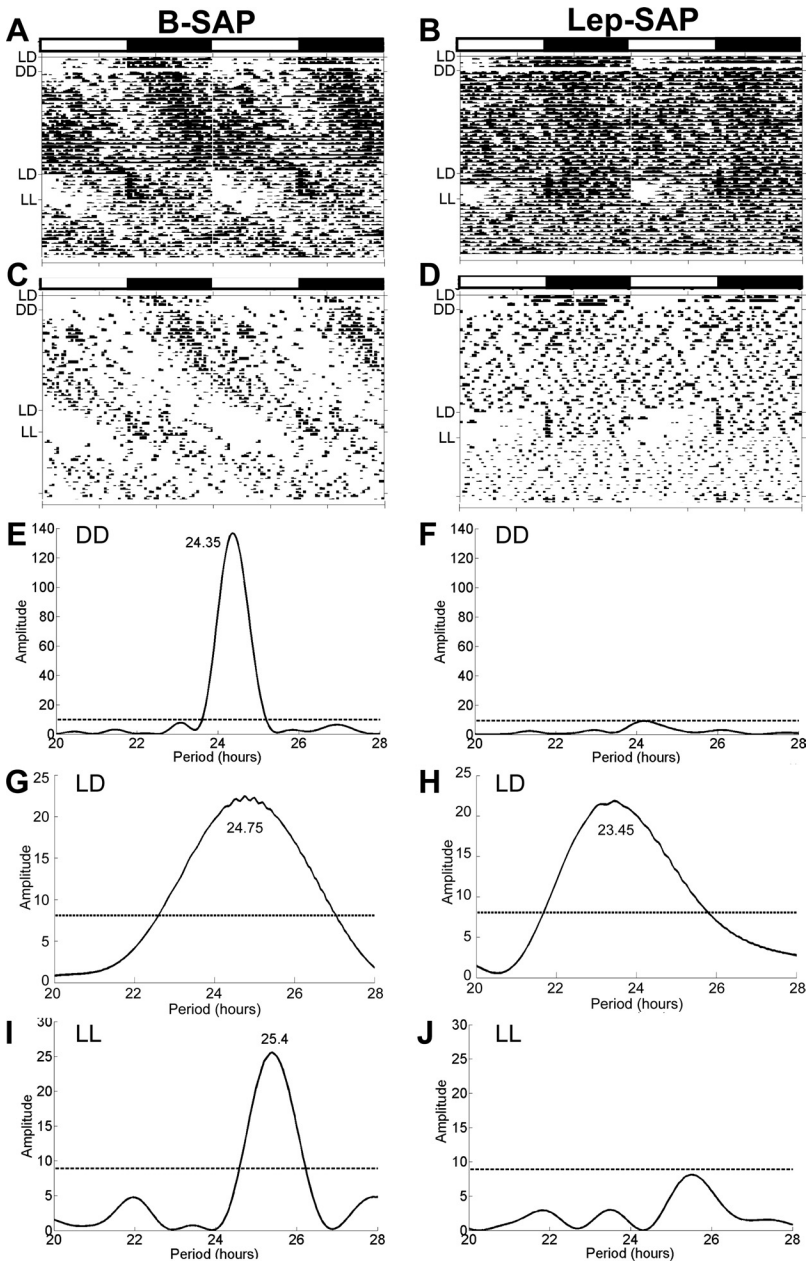

Fig. 6. Eatograms and Lomb-Scargle periodograms over 54 days during the static phase in Arc-injected Lep-SAP rats and in B-SAP rats. Data are shown for LD (3 days), DD (28 days), second LD (7 days), and LL (16 days). The white and black bars above the eatograms mark the light and dark periods during LD, respectively. *A* and *B*: batched eatograms for B-SAP ($n = 6$) and Lep-SAP ($n = 7$) groups, respectively. *C* and *D*: eatograms for a representative individual B-SAP or Lep-SAP rat. *E* and *F*: batched periodograms for DD. *G* and *H*: batched periodograms for second LD. *I* and *J*: batched periodograms for LL, respectively. Note that the tau in *G* includes the transition period from DD to LD, resulting in a tau that differs somewhat from the tau shown for this group in *E*. The dotted line represents the amplitude of a periodogram required for significance ($P < 0.05$).

capable of influencing certain aspects of feeding in these lesioned rats. Indeed, examination of the eatograms for Lep-SAP rats reveals acute changes in food intake occurring at the beginning of both the light and dark phases of the cycle. Therefore, it is reasonable to speculate that a direct effect of light, such as a masking (or aversive) effect (61), may have suppressed food intake during the light phase of the LD cycle in the Lep-SAP rats, giving the appearance of a circadian rhythm under those conditions during the static phase. As noted, this rhythm was not driven by a photically entrainable oscillator, such as those in the SCN, since the feeding rhythm itself was not entrained to the light-dark cycle, but dissipated immediately under continuous light or dark.

This study is the first to report the use of Lep-SAP to selectively destroy leptin receptor-expressing neurons in the brain. Injection of Lep-SAP into the Arc of S/D rats eliminated ~80% of Arc NPY/AGRP and α-MSH neurons, both known to express LepB-R (6, 55). In contrast, Lep-SAP did not reduce the numbers of AGRP or α-MSH neurons in the Arc of Zucker *fa/fa* rats, which express mutated low-affinity leptin receptors (96). In S/D rats, Lep-SAP also impaired feeding and body weight responses typically produced by leptin administration. These results demonstrate that Lep-SAP is both a selective and effective lesioning agent: its toxicity is primarily dependent on internalization of the LepR-B receptor; it destroys neuronal phenotypes known to express leptin receptors; and it impairs physiological responses mediated by leptin-sensitive neurons at the injection site.

In contrast to Arc injections, Lep-SAP injections into the adjacent VMN did not cause obesity or impair feeding rhythms under either LD or DD conditions. VMN injections greatly reduced SF-1 immunoreactive neurons in the VMN, where SF-1 is concentrated and coexpressed with LepR-B (22), while Arc

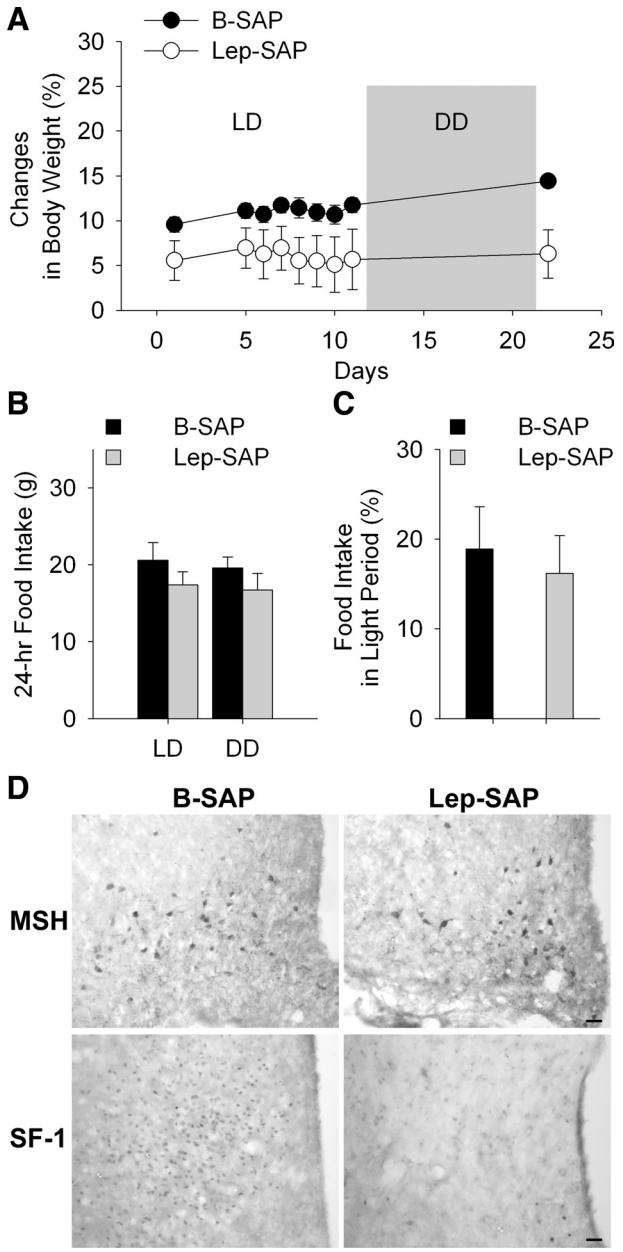

Fig. 7. Body weight and food intake and hypothalamic IHC in rats injected into the ventromedial nuclei of the hypothalamus (VMN) with B-SAP or Lep-SAP. *A–C*: body weight and food intake in VMN Lep-SAP and B-SAP rats. Body weight gain (*A*), shown as a percentage of body weight at the time of VMN injections. There was no difference in body weight between B-SAP ($n = 6$) and Lep-SAP ($n = 7$) rats at the time of surgery. Body weights and feeding are shown for two testing conditions, LD and DD (gray box in *A*), beginning 7 wk after the VMN injections. Lep-SAP rats weigh significantly less than B-SAPs across all test days ($P < 0.05$). Twenty-four-hour food intake (*B*) and percent of food intake during light period over daily intake (*C*) did not differ significantly between VMN B-SAP and Lep-SAP rats in LD. *D*: coronal sections of rat brain showing Arc and VMN in VMN B-SAP or Lep-SAP rats. The Arc sections were immunoreacted to reveal α-MSH cell bodies (*top*), which are localized to the Arc. The VMN sections were immunoreacted to reveal nuclei positive for SF-1, a peptide located within the VMN (*bottom*). Calibration bar = 20 μm.

LepR-B-expressing α-MSH neurons remained largely intact. Although not all SF-1 neurons were lesioned by our VMN injection, the fact that the same injection volume was used for both Arc and VMN injections makes it unlikely that the consequences of the Arc Lep-SAP injections were attributable to loss of VMN SF-1/LepR-B coexpressing neurons. This view and our results are consistent with the reports that disrupted activity rhythms resulting from loss of leptin receptors are restored when these receptors are reactivated only in the Arc (18). In addition, it is interesting to note that VMN Lep-SAP rats did not become obese or hyperphagic. This result is consistent with previous results using Cre-LoxP targeting in mice to destroy LepR-B receptors specifically on SF-1 expressing neurons. That treatment caused only mild obesity and did not produce hyperphagia (8, 22). From these data, we conclude that VMN neurons expressing LepR-B are not responsible for the loss of circadian rhythms of feeding we observed after Arc Lep-SAP injections.

Because of the established role of the SCN in generating circadian rhythms, the fact that SCN neurons express LepR-B (31, 55) and the fact that SCN lesions also produce loss of rhythms for feeding and RER (62, 63, and present findings), it is important to consider the possibility that the arrhythmic phenotype of Arc Lep-SAP rats was due to damage to both the SCN and Arc. However, this seems unlikely. First, the histological appearance of the SCN in Lep-SAP rats suggests that it remained intact. Second, anti-SAP IHC did not reveal uptake or presence of SAP immunoreactivity in the SCN after Arc-directed injections of Lep-SAP. If, indeed, lesioning of either structure were sufficient to produce arrhythmic feeding, this would suggest that both structures and their interactions are critical components for generation of circadian feeding rhythms. Lesion results, however, do not rule out the contribution of additional integrative sites to rhythm generation.

Neurons exhibiting robust circadian rhythms that would be potentially capable of controlling circadian feeding rhythms are present in the Arc (1, 32, 37, 54, 81). Not only do Arc leptin receptors exhibit diurnal variation (25), but Arc LepR-B-expressing neurons receive and appear to integrate food- and energy-related signals arising from diverse central and peripheral sites (9, 17, 45, 88, 95). For example, signaling by gastrin-releasing peptide has been reported to potently elevate the amplitude of Per2 circadian rhythm in the Arc but not in the SCN (37), suggesting that the integrative role of Arc neurons may shape their role as rhythm generators for food intake and enable them to coordinate and prioritize circadian controls of intake with homeostatic requirements. Furthermore, electrophysiological analyses and anatomical studies have revealed the presence of neural connections between the Arc and the SCN that might contribute to feeding rhythms (47, 59). More than 80% of both SCN and peri-SCN cells are responsive to Arc stimulation and ~13% of Arc cells contribute to the SCN/peri-SCN projection (76). Arc neurons contributing to this projection, some of which are sensitive to leptin, include POMC (42), galanin (2), and ghrelin (97). Thus, what is known of the anatomical connections of SCN and Arc is consistent with the hypothesis that feeding rhythms are generated by a circuitry that tightly couples that activity of these two sites. In addition to the SCN, Arc neurons innervate the dorsomedial hypothalamus (84), a proposed integrative site for circadian inputs from the SCN and metabolic cues arising from the Arc (77, 78).

Because Lep-SAP rats during the dynamic phase ate equal amounts during day and night and consumed 196% of control intake during the second week of rapid weight gain, masking of the endogenous feeding rhythm by hyperphagia may have occurred during the dynamic phase (89). In contrast, during the

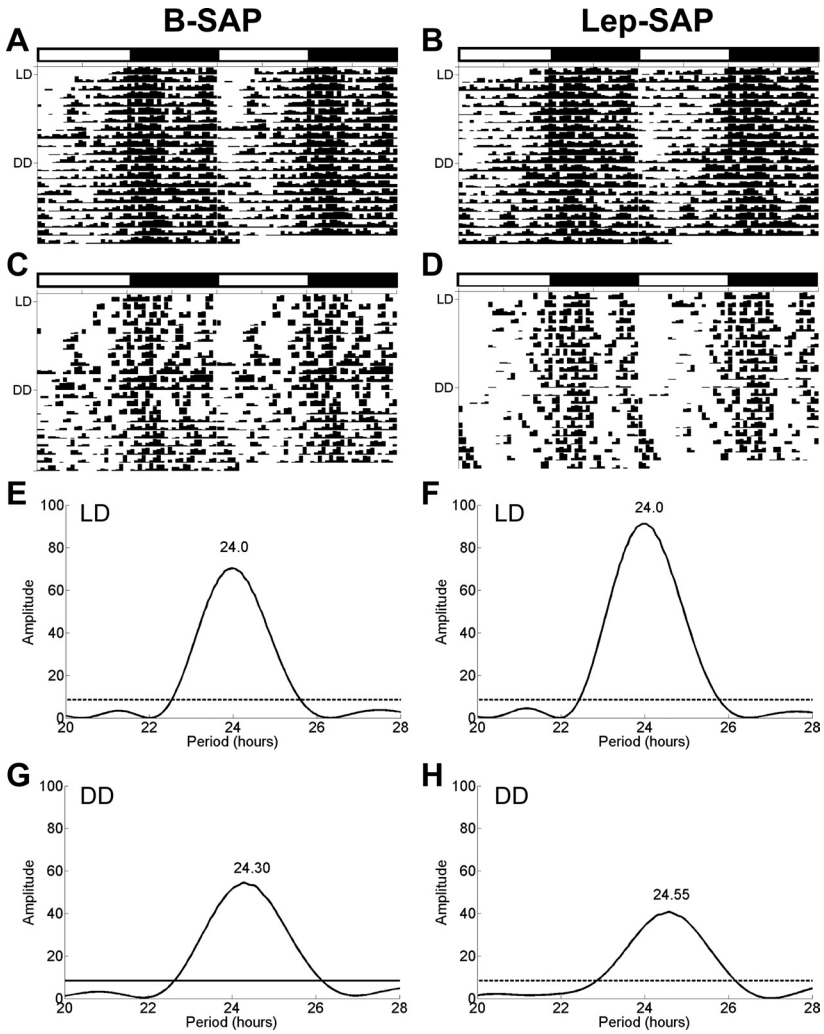

Fig. 8. Eatograms and Lomb-Scargle periodograms over 23 days in rats injected into the VMN with B-SAP or Lep-SAP. For the first 12 days, the rats were in 12:12-h LD and thereafter in DD. The white and black bars above the plots mark the light and dark periods during LD, respectively. *A* and *B*: batched eatograms for VMN B-SAP ($n = 6$) and Lep-SAP ($n = 7$) rats, respectively. *C* and *D*: eatograms for an individual VMN B-SAP and Lep-SAP rat. *E* and *F*: batched periodograms in LD. *G* and *H*: batched periodograms in DD. The dotted line in the periodograms indicates the required amplitude for statistical significance ($P < 0.05$).

static phase, hyperphagic masking seems an unlikely cause of arrhythmic feeding. During the static phase, 24-h food intake for Lep-SAP rats (26.3 ± 1.9 g) approached control levels (21.0 ± 1.3 g), and nighttime food intake was preferred under LD conditions (Table 1). Yet feeding remained arrhythmic under constant lighting conditions (both LL and DD) over the extended period of static phase analysis (several months). Thus, we suggest that if the circadian rhythm generator remains intact, hyperphagic masking might blunt, but not permanently eliminate, the circadian control of feeding. This leads us to interpret the apparently permanent loss of ad libitum feeding rhythms in Lep-SAP rats, as indicating that their lesion disabled the circadian feeding control circuitry.

It is important to acknowledge that feeding is subject to multiple controls, including homeostatic controls (26, 77) and that many of these appear to converge within the Arc (18, 45, 88). Therefore, it is unlikely that loss of circadian control is responsible for the entire Lep-SAP phenotype. Nevertheless, we note that *Clock* mutant mice are hyperphagic and obese with elevated daytime food intake (86) and that circadian disruption has been reported to cause both hyperphagia and obesity (7, 30, 41, 94). Thus, there is substantial support for the hypothesis that feeding arrhythmia observed after the Arc Lep-SAP lesion is due to specific loss of circadian control and is not secondary to hyperphagia or obesity. Nevertheless, recent data suggesting that obesity itself disrupts circadian rhythms of peripheral clock genes (40, 44, 48) are relevant to our present findings. Although these studies did not detect changes in clock genes in the MBH, our results suggesting that LepR-B-expressing neurons contribute to rhythm generation would, in fact, predict that obesity, which leads to leptin insensitivity, would reduce the effectiveness of leptin as a rhythm-generating mechanism. Certainly, however, obesity is not inextricably linked to arrhythmic feeding, as the present results illustrate. Feeding rhythms in our experiments were disrupted by both SCN and Lep-SAP Arc lesions, with lesion of one site associated with weight loss and the other with extreme obesity.

Obese Zucker rats, which lack functional leptin receptors, and rats with VMH-area lesions that include the Arc (5, 60) become obese, but consistent with our static-phase results, these rats maintain circadian rhythms of feeding in LD (3, 27, 29, 58). These findings would seem to challenge our conclusions that Arc LepR-B-expressing neurons are significant contributors to generation of feeding rhythms. However, two important points are noteworthy. First, in Zucker *fa/fa* rats, other inputs to neurons expressing the mutated leptin receptor, that would not be present in the lesioned rat, could presumably continue to function as rhythm generators. Secondly, it is also important to note that it is not entirely clear that circadian

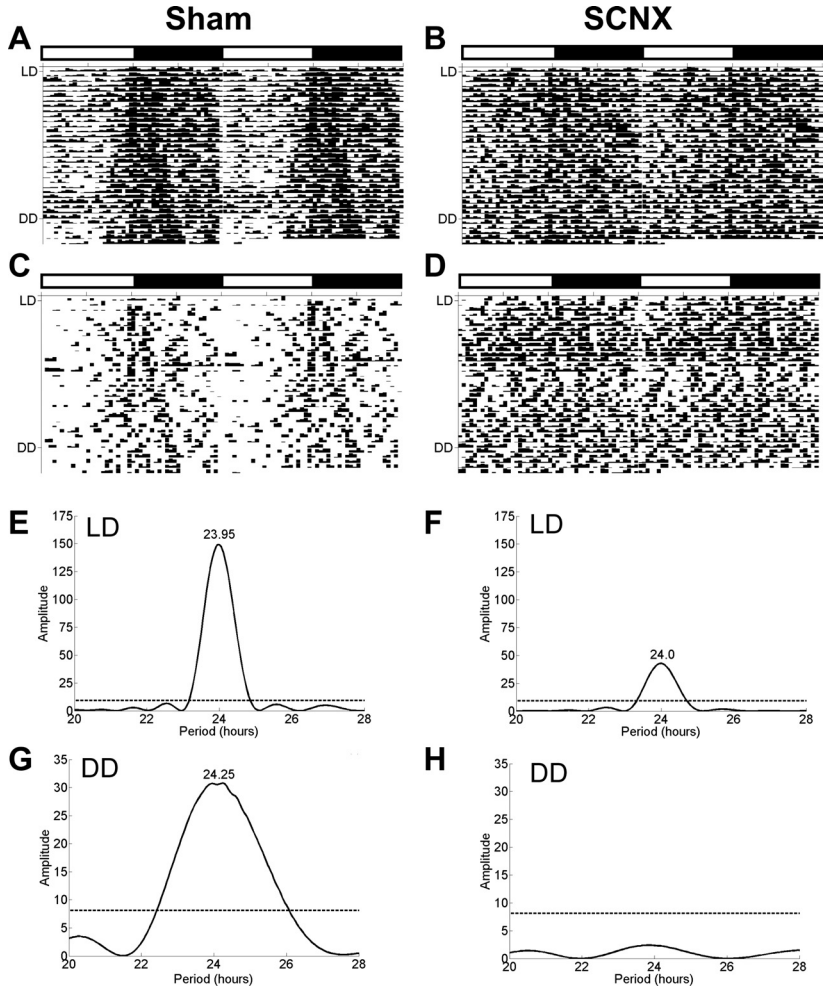

Fig. 9. Eatograms and Lomb-Scargle periodograms for rats with lesions of SCN (SCNX) or sham lesion. For the first 25 days, the rats were in 12:12-h LD and thereafter for 5 days in DD. The white and black bars above the plots mark the light and dark periods during LD. *A* and *B*: batched eatograms for sham ($n = 6$) and SCNX ($n = 7$) rats, respectively. *C* and *D*: eatogram for an individual sham and SCNX rat. *E* and *F*: batched periodograms for LD. *G* and *H*: batched periodograms for DD. The dotted line in the periodograms indicates the required amplitude for statistical significance ($P < 0.05$).

feeding rhythms remain intact in either Zucker *fa/fa* or VMH-lesioned rats, since they have not been examined in the extended absence of photic cues as is necessary for observation of significant repetitive cycles. As we observed in the present study, absence of a circadian rhythm of feeding is not necessarily associated with loss of a nocturnal feeding pattern in LD.

These experiments confirm that ad libitum feeding in rats has an endogenous circadian rhythm, as previously inferred from raster plots, LD feeding niche preferences and other data (10, 49, 56–58, 60, 64, 68, 71–75, 80, 87, 92, 98). However, our findings also demonstrate that circadian rhythms of feeding cannot be determined from LD measures alone but must also be studied under constant illumination (LL or DD). Use of both raster plots and periodograms combined with appropriate experimental design enables detection of valid rhythms and proper interpretation of disrupted rhythms (70).

Our work suggests that both the Arc and the SCN are required for generation and maintenance of endogenous feeding rhythms and for entrainment of these rhythms to the LD cycle. These findings are supported by work showing, respectively, that the Arc contains molecular clocks (1) that are reset in response to restricted meals (54) or fasting (32) and by the well-established finding that the SCN contains clocks that respond to photic cues. These results, therefore, add to the Arc's many roles an underappreciated functional circadian relationship with the SCN (60, 68, 78), as well as revealing an essential role for the Arc in maintaining circadian rhythms of ad libitum feeding independent of light entrainment.

Perspectives and Significance

Demonstration that circadian rhythms of ad libitum feeding require both the SCN and the leptin-sensitive network of the Arc suggests an important but neglected interaction between these two nuclei in rhythm generation. The anatomical circuitry mediating this interaction and the specific role of endogenous oscillators within the Arc require further elaboration. A more complete appreciation of the contributions of leptin, hyperphagia, and obesity in rhythm dysfunction will be of value in understanding pathological states such as metabolic diseases and diabetes that are associated with altered rhythms (53).

GRANTS

This work was supported by Public Health Service Grants DK-40498 and DK-81546 to S. Ritter and DA-023202 to H. T. Jansen.

DISCLOSURES

No conflicts of interest, financial or otherwise, are declared by the authors.

AUTHOR CONTRIBUTIONS

Author contributions: A.-J.L., M.F.W., and S.R. conception and design of research; A.-J.L., M.F.W., M.T.O., B.R.S., Q.W., T.T.D., and B.L.R. per-

formed experiments; A.-J.L., M.F.W., and H.T.J. analyzed data; A.-J.L., M.F.W., and S.R. interpreted results of experiments; A.-J.L. and M.F.W. prepared figures; A.-J.L. drafted manuscript; A.-J.L., M.F.W., H.T.J., and S.R. edited and revised manuscript; A.-J.L., M.F.W., and S.R. approved final version of manuscript.

REFERENCES

1. **Abe M, Herzog ED, Yamazaki S, Straume M, Tei H, Sakaki Y, Menaker M, Block GD.** Circadian rhythms in isolated brain regions. *J Neurosci* 22: 350–356, 2002.
2. **Abrahamson EE, Moore RY.** Suprachiasmatic nucleus in the mouse: retinal innervation, intrinsic organization and efferent projections. *Brain Res* 916: 172–191, 2001.
3. **Alingh Prins A, de Jong-Nagelsmit A, Keijser J, Strubbe JH.** Daily rhythms of feeding in the genetically obese and lean Zucker rats. *Physiol Behav* 38: 423–426, 1986.
4. **Anand BK, Brobeck JR.** Hypothalamic controls of food intake in rats and cats. *Yale J Biol Med* 24: 123–140, 1951.
5. **Balagura S, Devenport LD.** Feeding patterns of normal and ventromedial hypothalamic lesioned male and female rats. *J Comp Physiol Psychol* 71: 357–364, 1970.
6. **Baskin DG, Schwartz MW, Seeley RJ, Woods SC, Porte D, Jr, Breininger JF, Jonak Z, Schaefer J, Krouse M, Burghardt C, Campfield LA, Burn P, Kochan JP.** Leptin receptor long-form splice-variant protein expression in neuron cell bodies of the brain and co-localization with neuropeptide Y mRNA in the arcuate nucleus. *J Histochem Cytochem* 47: 353–362, 1999.
7. **Bass J, Takahashi JS.** Circadian integration of metabolism and energetics. *Science* 330: 1349–1354, 2010.
8. **Bingham NC, Anderson KK, Reuter AL, Stallings NR, Parker KL.** Selective loss of leptin receptors in the ventromedial hypothalamic nucleus results in increased adiposity and a metabolic syndrome. *Endocrinology* 149: 2138–2148, 2008.
9. **Blevins JE, Baskin DG.** Hypothalamic-brainstem circuits controlling eating. *Forum Nutr* 63: 133–140, 2010.
10. **Borbely AA, Neuhaus HU.** Daily pattern of sleep, motor activity and feeding in the rat: effects of regular and gradually extended photoperiods. *J Comp Physiol* 124: 1–14, 1978.
11. **Brobeck JR, Tepperman J, Long CNH.** Experimental hypothalamic hyperphagia in the albino rat. *Yale J Biol Med* 15: 831–853, 1943.
12. **Brooks CM, Lambert HF.** A study of the effect of limitation of food intake and the method of feeding on the rate of weight gain during hypothalamic obesity in the albino rat. *Am J Physiol* 147: 695–707, 1946.
13. **Bugarith K, Dinh TT, Li AJ, Speth RC, Ritter S.** Basomedial hypothalamic injections of neuropeptide Y conjugated to saporin selectively disrupt hypothalamic controls of food intake. *Endocrinology* 146: 1179–1191, 2005.
14. **Buijs RM, Scheer FA, Kreier F, Yi C, Bos N, Goncharuk VD, Kalsbeek A.** Organization of circadian functions: interaction with the body. *Prog Brain Res* 153: 341–360, 2006.
15. **Choi S, Sparks R, Clay M, Dallman MF.** Rats with hypothalamic obesity are insensitive to central leptin injections. *Endocrinology* 140: 4426–4433, 1999.
16. **Chua SC Jr,.** White DW, Wu-Peng XS, Liu SM, Okada N, Kershaw EE, Chung WK, Power-Kehoe L, Chua M, Tartaglia LA, and Leibel RL. Phenotype of fatty due to Gln269Pro mutation in the leptin receptor (Lepr). *Diabetes* 45: 1141–1143, 1996.
17. **Cone RD, Cowley MA, Butler AA, Fan W, Marks DL, Low MJ.** The arcuate nucleus as a conduit for diverse signals relevant to energy homeostasis. *Int J Obes Relat Metab Disord* 25 *Suppl* 5: S63–S67, 2001.
18. **Coppari R, Ichinose M, Lee CE, Pullen AE, Kenny CD, McGovern RA, Tang V, Liu SM, Ludwig T, Chua SC Jr, Lowell BB, Elmquist JK.** The hypothalamic arcuate nucleus: a key site for mediating leptin's effects on glucose homeostasis and locomotor activity. *Cell Metab* 1: 63–72, 2005.
19. **da Silva BA, Bjorbak C, Uotani S, Flier JS.** Functional properties of leptin receptor isoforms containing the Gln→Pro extracellular domain mutation of the fatty rat. *Endocrinology* 139: 3681–3690, 1998.
20. **Danguir J, Nicolaidis S.** Sleep and feeding patterns in the ventromedial hypothalamic lesioned rat. *Physiol Behav* 21: 769–777, 1978.
21. **Dawson R, Pelleymounter MA, Millard WJ, Liu S, Eppler B.** Attenuation of leptin-mediated effects by monosodium glutamate-induced arcuate nucleus damage. *Am J Physiol Endocrinol Metab* 273: E202–E206, 1997.
22. **Dhillon H, Zigman JM, Ye C, Lee CE, McGovern RA, Tang V, Kenny CD, Christiansen LM, White RD, Edelstein EA, Coppari R, Balthasar N, Cowley MA, Chua Jr. S, Elmquist JK, Lowell BB.** Leptin directly activates SF1 neurons in the VMH, and this action by leptin is required for normal body-weight homeostasis. *Neuron* 49: 191–203, 2006.
23. **Dube MG, Xu B, Kalra PS, Sninsky CA, Kalra SP.** Disruption in neuropeptide Y and leptin signaling in obese ventromedial hypothalamic-lesioned rats. *Brain Res* 816: 38–46, 1999.
24. **Eastman C, Rechtschaffen A.** Circadian temperature and wake rhythms of rats exposed to prolonged continuous illumination. *Physiol Behav* 31: 417–427, 1983.
25. **Ellis C, Moar KM, Logie TJ, Ross AW, Morgan PJ, Mercer JG.** Diurnal profiles of hypothalamic energy balance gene expression with photoperiod manipulation in the Siberian hamster, *Phodopus sungorus*. *Am J Physiol Regul Integr Comp Physiol* 294: R1148–R1153, 2008.
26. **Elmquist JK, Coppari R, Balthasar N, Ichinose M, Lowell BB.** Identifying hypothalamic pathways controlling food intake, body weight, and glucose homeostasis. *J Comp Neurol* 493: 63–71, 2005.
27. **Enns MP, Grinker JA.** Dietary self-selection and meal patterns of obese and lean Zucker rats. *Appetite* 4: 281–293, 1983.
28. **Friedman JM, Halaas JL.** Leptin and the regulation of body weight in mammals. *Nature* 395: 763–770, 1998.
29. **Fukagawa K, Sakata T, Yoshimatsu H, Fujimoto K, Uchimura K, Asano C.** Advance shift of feeding circadian rhythm induced by obesity progression in Zucker rats. *Am J Physiol Regul Integr Comp Physiol* 263: R1169–R1175, 1992.
30. **Garaulet M, Ordovas JM, Madrid JA.** The chronobiology, etiology and pathophysiology of obesity. *Int J Obes (Lond)* 34: 1667–1683, 2010.
31. **Guan XM, Hess JF, Yu H, Hey PJ, van der Ploeg LH.** Differential expression of mRNA for leptin receptor isoforms in the rat brain. *Mol Cell Endocrinol* 133: 1–7, 1997.
32. **Guilding C, Hughes AT, Brown TM, Namvar S, Piggins HD.** A riot of rhythms: neuronal and glial circadian oscillators in the mediobasal hypothalamus. *Mol Brain* 2: 28, 2009.
33. **Hasek BE, Stewart LK, Henagan TM, Boudreau A, Lenard NR, Black C, Shin J, Huypens P, Malloy VL, Plaisance EP, Krajcik RA, Orentreich N, Gettys TW.** Dietary methionine restriction enhances metabolic flexibility and increases uncoupled respiration in both fed and fasted states. *Am J Physiol Regul Integr Comp Physiol* 299: R728–R739, 2010.
34. **Hastings MH, Reddy AB, Maywood ES.** A clockwork web: circadian timing in brain and periphery, in health and disease. *Nat Rev Neurosci* 4: 649–661, 2003.
35. **Hetherington AW.** The relation of various hypothalamic lesions to adiposity and other phenomena in the rat. *Am J Physiol* 133: 326–327, 1941.
36. **Ho A, Chin A.** Circadian feeding and drinking patterns of genetically obese mice fed solid chow diet. *Physiol Behav* 43: 651–656, 1988.
37. **Hughes AT, Guilding C, Piggins HD.** Neuropeptide signaling differentially affects phase maintenance and rhythm generation in SCN and extra-SCN circadian oscillators. *PLos One* 6: e18926, 2011.
38. **Jansen HT, Sergeeva A, Stark G, Sorg BA.** Circadian discrimination of reward: Evidence for simultaneous yet separable food- and drug-entrained rhythms in the rat. *Chronobiol Int* In press.
39. **Kakolewski JW, Deaux E, Christensen J, Case B.** Diurnal patterns in water and food intake and body weight changes in rats with hypothalamic lesions. *Am J Physiol* 221: 711–718, 1971.
40. **Kaneko K, Yamada T, Tsukita S, Takahashi K, Ishigaki Y, Oka Y, Katagiri H.** Obesity alters circadian expressions of molecular clock genes in the brainstem. *Brain Res* 1263: 58–68, 2009.
41. **Karatsoreos IN, Bhagat S, Bloss EB, Morrison JH, McEwen BS.** Disruption of circadian clocks has ramifications for metabolism, brain, and behavior. *Proc Natl Acad Sci USA* 108: 1657–1662, 2011.
42. **Kineman RD, Kraeling RR, Crim JW, Leshin LS, Barb CR, Rampacek GB.** Localization of proopiomelanocortin (POMC) immunoreactive neurons in the forebrain of the pig. *Biol Reprod* 40: 1119–1126, 1989.
43. **King BM.** The rise, fall, and resurrection of the ventromedial hypothalamus in the regulation of feeding behavior and body weight. *Physiol Behav* 87: 221–244, 2006.
44. **Kohsaka A, Laposky AD, Ramsey KM, Estrada C, Joshu C, Kobayashi Y, Turek FW, Bass J.** High-fat diet disrupts behavioral and molecular circadian rhythms in mice. *Cell Metab* 6: 414–421, 2007.
45. **Konner AC, Klockener T, Bruning JC.** Control of energy homeostasis by insulin and leptin: targeting the arcuate nucleus and beyond. *Physiol Behav* 97: 632–638, 2009.

46. **Kopelman P, Caterson I, Dietz W.** *Clinical Obesity in Adults and Children*. Chichester, UK: John Wiley & Sons, 2009.
47. **Krout KE, Kawano J, Mettenleiter TC, Loewy AD.** CNS inputs to the suprachiasmatic nucleus of the rat. *Neuroscience* 110: 73–92, 2002.
48. **Kudo T, Akiyama M, Kuriyama K, Sudo M, Moriya T, Shibata S.** Night-time restricted feeding normalises clock genes and Pai-1 gene expression in the *db/db* mouse liver. *Diabetologia* 47: 1425–1436, 2004.
49. **Le Magnen J, Tallon S.** The spontaneous periodicity of ad libitum food intake in white rats. *J Physiol (Paris)* 58: 323–349, 1966.
50. **Leveille GA, O'Hea EK.** Influence of periodicity of eating on energy metabolism in the rat. *J Nutr* 93: 541–545, 1967.
51. **Li AJ, Wang Q, Dinh TT, Ritter S.** Simultaneous silencing of Npy and Dbh expression in hindbrain A1/C1 catecholamine cells suppresses glucoprivic feeding. *J Neurosci* 29: 280–287, 2009.
52. **Li AJ, Wang Q, Ritter S.** Differential responsiveness of dopamine-beta-hydroxylase gene expression to glucoprivation in different catecholamine cell groups. *Endocrinology* 147: 3428–3434, 2006.
53. **Maury E, Ramsey KM, Bass J.** Circadian rhythms and metabolic syndrome: from experimental genetics to human disease. *Circ Res* 106: 447–462.
54. **Mendoza J, Pevet P, Felder-Schmittbuhl MP, Bailly Y, Challet E.** The cerebellum harbors a circadian oscillator involved in food anticipation. *J Neurosci* 30: 1894–1904, 2010.
55. **Mercer JG, Hoggard N, Williams LM, Lawrence CB, Hannah LT, Trayhurn P.** Localization of leptin receptor mRNA and the long form splice variant (Ob-Rb) in mouse hypothalamus and adjacent brain regions by in situ hybridization. *FEBS Lett* 387: 113–116, 1996.
56. **Millan MJ, Millan MH, Reid LD, Herz A.** The role of the mediobasal arcuate hypothalamus in relation to opioid systems in the control of ingestive behaviour in the rat. *Brain Res* 381: 29–42, 1986.
57. **Mistlberger RE, Antle MC.** Neonatal monosodium glutamate alters circadian organization of feeding, food anticipatory activity and photic masking in the rat. *Brain Res* 842: 73–83, 1999.
58. **Mistlberger RE, Lukman H, Nadeau BG.** Circadian rhythms in the Zucker obese rat: assessment and intervention. *Appetite* 30: 255–267, 1998.
59. **Moga MM, Moore RY.** Organization of neural inputs to the suprachiasmatic nucleus in the rat. *J Comp Neurol* 389: 508–534, 1997.
60. **Moore-Ede M, Sulzman F, Fuller C.** *The Clocks That Time Us: Physiology of the Circadian Timing System*. Cambridge, MA: Harvard University Press, 1982.
61. **Mrosovsky N.** Masking: history, definitions, and measurement. *Chronobiol Int* 16: 415–429, 1999.
62. **Nagai K, Nishio T, Nakagawa H.** Bilateral lesions of suprachiasmatic nucleus eliminate circadian rhythms of oxygen consumption and the respiratory quotient in rats. *Experientia* 41: 1136–1138, 1985.
63. **Nagai K, Nishio T, Nakagawa H, Nakamura S, Fukuda Y.** Effect of bilateral lesions of the suprachiasmatic nuclei on the circadian rhythm of food-intake. *Brain Res* 142: 384–389, 1978.
64. **Nakagawa H, Okumura N.** Coordinated regulation of circadian rhythms and homeostasis by the suprachiasmatic nucleus. *Proc Jpn Acad Ser B Phys Biol Sci* 86: 391–409, 2010.
65. **Paxinos G, Watson C.** *The Rat Brain in Stereotaxic Coordinates*. San Diego, CA: Academic Press, 2007.
66. **Phillips MS, Liu Q, Hammond HA, Dugan V, Hey PJ, Caskey CJ, Hess JF.** Leptin receptor missense mutation in the fatty Zucker rat. *Nat Genet* 13: 18–19, 1996.
67. **Piccione G, Caola G, Refinetti R.** Feeble weekly rhythmicity in hematological, cardiovascular, and thermal parameters in the horse. *Chronobiol Int* 21: 571–589, 2004.
68. **Refinetti R.** *Circadian Physiology.* Boca Raton, FL: CRC Press, 2006.
69. **Refinetti R.** Metabolic heat production, heat loss and the circadian rhythm of body temperature in the rat. *Exp Physiol* 88: 423–429, 2003.
70. **Refinetti R, CornelissonHalberg F.** Procedures for numerical analysis of circadian rhythms. *Biol Rhythms Res* 38: 275–325, 2007.
71. **Richter CP.** Animal behavior and internal drives. *Q Rev Biol* 2: 307–343, 1927.
72. **Richter CP.** *Biological Clocks in Medicine and Psychiatry*. Springfield, Illinois: C. C. Thomas, 1965.
73. **Rietveld WJ, Hoor FT, Kooij M, Flory W.** Maintenance of 24 hour eating rhythmicity during gold thioglucose induced hypothalamic hyperphagia in rats. *Physiol Behav* 22: 549–553, 1979.
74. **Rietveld WJ, Ten Hoor F, Kooij M, Flory W.** Changes in 24-hour fluctuations of feeding behavior during hypothalamic hyperphagia in rats. *Physiol Behav* 21: 615–622, 1978.
75. **Rosenwasser AM, Boulos Z, Terman M.** Circadian organization of food intake and meal patterns in the rat. *Physiol Behav* 27: 33–39, 1981.
76. **Saeb-Parsy K, Lombardelli S, Khan FZ, McDowall K, Au-Yong IT, Dyball RE.** Neural connections of hypothalamic neuroendocrine nuclei in the rat. *J Neuroendocrinol* 12: 635–648, 2000.
77. **Saper CB.** Staying awake for dinner: hypothalamic integration of sleep, feeding, and circadian rhythms. *Prog Brain Res* 153: 243–252, 2006.
78. **Saper CB, Scammell TE, Lu J.** Hypothalamic regulation of sleep and circadian rhythms. *Nature* 437: 1257–1263, 2005.
79. **Scislowski PW, Tozzo E, Zhang Y, Phaneuf S, Prevelige R, Cincotta AH.** Biochemical mechanisms responsible for the attenuation of diabetic and obese conditions in ob/ob mice treated with dopaminergic agonists. *Int J Obes Relat Metab Disord* 23: 425–431, 1999.
80. **Selmaoui B, Waterhouse J, Thibault L.** Ingestive pattern changes in blinded rat. *Biol Rhythm Res* 34: 397–411, 2004.
81. **Shieh KR.** Distribution of the rhythm-related genes rPERIOD1, rPERIOD2, and rCLOCK, in the rat brain. *Neuroscience* 118: 831–843, 2003.
82. **Strohmayer AJ, Smith GP.** The meal pattern of genetically obese (*ob/ob*) mice. *Appetite* 8: 111–123, 1987.
83. **Tepperman J, Brobeck JR, Long CN.** The effects of hypothalamic hyperphagia and of alterations in feeding habits on the metabolism of the albino rat. *Yale J Biol Med* 15: 855–874, 1943.
84. **Thompson RH, Swanson LW.** Organization of inputs to the dorsomedial nucleus of the hypothalamus: a reexamination with Fluorogold and PHAL in the rat. *Brain Res Brain Res Rev* 27: 89–118, 1998.
85. **Tsutsumi K, Inoue Y, Kondo Y.** The relationship between lipoprotein lipase activity and respiratory quotient of rats in circadian rhythms. *Biol Pharm Bull* 25: 1360–1363, 2002.
86. **Turek FW, Joshu C, Kohsaka A, Lin E, Ivanova G, McDearmon E, Laposky A, Losee-Olson S, Easton A, Jensen DR, Eckel RH, Takahashi JS, Bass J.** Obesity and metabolic syndrome in circadian Clock mutant mice. *Science* 308: 1043–1045, 2005.
87. **Van den Pol AN, Powley T.** A fine-grained anatomical analysis of the role of the rat suprachiasmatic nucleus in circadian rhythms of feeding and drinking. *Brain Res* 160: 307–326, 1979.
88. **van den Top M, Spanswick D.** Integration of metabolic stimuli in the hypothalamic arcuate nucleus. *Prog Brain Res* 153: 141–154, 2006.
89. **Van Dongen HPA, Dinges DF.** *Circadian Rhythms in Fatigue, Alertness and Performance*. Philadelphia, PA: W. B. Saunders, 2000.
90. **Vieira E, Nilsson EC, Nerstedt A, Ormestad M, Long YC, Garcia-Roves PM, Zierath JR, Mahlapuu M.** Relationship between AMPK and the transcriptional balance of clock-related genes in skeletal muscle. *Am J Physiol Endocrinol Metab* 295: E1032–E1037, 2008.
91. **Watts AG, Swanson LW, Sanchez-Watts G.** Efferent projections of the suprachiasmatic nucleus: I. Studies using anterograde transport of *Phaseolus vulgaris* leucoagglutinin in the rat. *J Comp Neurol* 258: 204–229, 1987.
92. **Wiepkema PR, de Ruiter L, Reddingius J.** Circadian rhythms in the feeding behaviour of CBA mice. *Nature* 209: 935–936, 1966.
93. **Wiley RG, Kline IR.** Neuronal lesioning with axonally transported toxins. *J Neurosci Methods* 103: 73–82, 2000.
94. **Williams DL, Schwartz MW.** Out of synch: Clock mutation causes obesity in mice. *Cell Metab* 1: 355–356, 2005.
95. **Williams KW, Scott MM, Elmquist JK.** From observation to experimentation: leptin action in the mediobasal hypothalamus. *Am J Clin Nutr* 89: 985S–990S, 2009.
96. **Yamashita T, Murakami T, Iida M, Kuwajima M, Shima K.** Leptin receptor of Zucker fatty rat performs reduced signal transduction. *Diabetes* 46: 1077–1080, 1997.
97. **Yi CX, van der Vliet J, Dai J, Yin G, Ru L, Buijs RM.** Ventromedial arcuate nucleus communicates peripheral metabolic information to the suprachiasmatic nucleus. *Endocrinology* 147: 283–294, 2006.
98. **Yoshihara T, Honma S, Mitome M, Honma K.** Independence of feeding-associated circadian rhythm from light conditions and meal intervals in SCN lesioned rats. *Neurosci Lett* 222: 95–98, 1997.
99. **Zhang Y, Proenca R, Maffei M, Barone M, Leopold L, Friedman JM.** Positional cloning of the mouse obese gene and its human homologue. *Nature* 372: 425–432, 1994.